ELSEVIER

Nuclear Physics A 577 (1994) 585–604

NUCLEAR PHYSICS A

Tests and predictions of new effective interactions in the 0f1p shell

W.A. Richter [a], M.G. Van der Merwe [a], R.E. Julies [b], B.A. Brown [c]

[a] *Physics Department, University of Stellenbosch, Stellenbosch 7600, South Africa*

[b] *Physics Department, University of the Western Cape, Private Bag X17, Bellville, C.P. 7530, South Africa*

[c] *National Superconducting Cyclotron Laboratory and Department of Physics and Astronomy, Michigan State University, East Lansing, MI 48824, USA*

Received 29 December 1993; revised 12 April 1994

Abstract

New two-body interactions were derived recently for nuclei in the lower part of the 0f1p shell ($A = 41$–49) by fitting a semi-empirical potential form, known as a modified surface one-boson exchange potential (MSOBEP), and also two-body matrix elements, to 61 binding energy data. The wave functions based on these interactions are now used to calculate spectroscopic factors, B(E2) and B(M1) transition rates, and Gamow–Teller strengths in the full 0f1p model space. Comprehensive comparisons with available experimental data are made to assess the quality of the wave functions. Good agreement between experiment and the calculated observables is generally found, which indicates that the new interactions are reliable approximations to the effective interaction in the 0f1p shell.

1. Introduction

The shell-model calculations leading to the wave functions used in the present study were fully discussed in a previous paper [1]. In these calculations two methods were used to derive effective interactions from fits to energy level data. In the first method, a semi-empirical interaction based on one-boson exchange potentials (OBEP) plus core polarization correction terms of the multipole–multipole type, was fitted to 61 binding and excitation energies in the mass range $A = 41$–49. Other refinements to the interaction such as the inclusion of a density dependence, and a mass dependence of the two-body matrix elements, were also employed. After several iterations an r.m.s. deviation of 176 keV was obtained with a ten-parameter fit (including four single-particle energies). The final interaction was called FPD6 (see Table 3 of Ref. [1]), and may be considered

0375-9474/94/$07.00
SSDI 0375-9474(94)00224-B

to have a modified surface one-boson exchange potential (MSOBEP) form. A similar semi-empirical interaction was successfully used by Brown et al. [2] in the 1s0d shell.

In the second method a model-independent (MI) method was used to fit 12 linear combinations of single-particle energies and two-body matrix elements to the same data, while constraining the remaining two-body matrix elements to values of the renormalized Kuo–Brown G-matrix interaction. The final fit yielded an r.m.s. deviation of 163 keV, and the interaction was called FPMI3 (see Table 3 of Ref. [1]).

The fact that the wave functions based on the new interactions reproduced experimental level spectra and measured ground-state magnetic dipole and quadrupole moments of nuclei from mass 41 to 49 very well [1], prompted the present comprehensive calculations of spectroscopic factors, $B(\mathrm{M1})$ and $B(\mathrm{E2})$ transition rates, and Gamow–Teller strengths in the same mass range. These calculations are intended to serve as more sensitive tests of the wave functions. The similarity of the model-dependent FPD6 and model-independent FPMI3 interactions makes it unnecessary to include the results for both interactions here. Only those for FPD6 are given, and significant differences between the results for the two interactions will be mentioned. In addition, the FPD6 interaction was shown in our previous work to produce better results for $A = 48$ and 49, and is thus favoured over the FPMI3 interaction.

Calculated wave functions

The calculations assume a ^{40}Ca core and the complete set of basis states which can be generated from the four orbits of the 0f1p shell. For the Ca isotopes up to ^{48}Ca the calculated ground-state wave functions are predominantly $f^n_{7/2}$. A typical case is ^{44}Ca where the wave function is (only components greater than 3% indicated) 82.8% $f^4_{7/2}$ and 7.5% $f^2_{7/2}p^2_{3/2}$. For the ground states of the Sc and Ti isotopes there are in general larger admixtures of the $p_{3/2}$, $f_{5/2}$, $p_{1/2}$ components than in Ca. For example, in ^{44}Sc the largest components of the ground-state wave function are 56.4% $f^4_{7/2}$, 12.8% $f^3_{7/2}p^1_{3/2}$, 9.4% $f^3_{7/2}f^1_{5/2}$, 8.2% $f^2_{7/2}p^2_{3/2}$ and 3.5% $f^2_{7/2}f^2_{5/2}$.

For the FPMI3 interaction the occupation numbers for $A = 41$–45 are very similar to those of FPD6, differing typically by only a few per cent in most cases. However, for the Ca isotopes in the mass range 47 to 49, there are more significant differences, particularly for some excited states.

2. Spectroscopic factors for transfer to $A = 41$–49 nuclei

Spectroscopic factors for single-nucleon transfer reactions depend on the wave functions of both the initial and final states. A comparison between theory and experiment for spectroscopic factors therefore provides an essential test of the wave functions.

The wave functions produced by the OXBASH [3] shell-model code are calculated in the uncoupled m-scheme representation and the program utilizes the occupation number

representation. The spectroscopic factor for stripping between states $|J_iT_i\rangle$ and $|J_fT_f\rangle$, where i and f represent the initial and final states, respectively, is given in the second-quantization formalism [4,5] as:

$$S^+_{l,j} = \frac{|\langle A+1; J_fT_f|||a^+_{lj}|||A; J_iT_i\rangle|^2}{(2J_f+1)(2T_f+1)}, \tag{1}$$

where the matrix element has been reduced with respect to both spin and isospin, and a^+_{lj} is the operator which creates a nucleon with quantum numbers l and j. Eq. (1) is valid for both the stripping and pickup reaction provided that f and i are applied to the heavy and light nuclei, respectively.

The quantity $C^2S_{l,j}$ is extracted experimentally, with C the isospin vector coupling coefficient:

$$C = \langle T_iT_{iz}; tm_t|T_fT_{fz}\rangle. \tag{2}$$

Since the j-dependence of the measured transfer cross sections can usually not be determined, the extracted spectroscopic factors depend only on the orbital angular momentum. The measured value is then compared with the prediction $S_l = \sum_j S_{lj}$.

When comparing the shell-model spectroscopic factors calculated with the wave functions based on the FPD6 interaction with experimental spectroscopic factors, we shall be concerned with:

$$S(l=3) \equiv S(f_{7/2}) + S(f_{5/2}), \tag{3}$$

and with:

$$S(l=1) \equiv S(p_{3/2}) + S(p_{1/2}). \tag{4}$$

2.1. Comparison of spectroscopic factors

In Tables 1 to 4 our calculated spectroscopic factors for the FPD6 interaction are compared with experimental values and with values obtained from other shell-model calculations. The contributions for the $f_{7/2}$ and $p_{3/2}$ subshells are also shown. The generally weaker contributions for the $f_{5/2}$ and $p_{1/2}$ subshells can be obtained by subtraction from the sums for $l = 3$ and 1, respectively. For most transfer reactions to masses 42 to 44 a "best set" of experimental spectroscopic factors from the compilation by Endt [4], in which all values were recalculated with the same set of normalization constants and then averaged, was used. Individual measurements in this set have been assigned a 25% experimental error. For masses 45 to 49 values from more recent Nuclear Data Sheets [6–8] have mainly been used.

The theoretical spectroscopic factors are taken from McGrory et al. [9], Olsen and Osnes [10], Cole [11,12] and McGrory [15]. The values of Olsen and Osnes for $A = 43$ were calculated (i) in a complete $(fp)^3$ model space with a realistic effective interaction based on the bare G-matrix interaction of Kuo and Brown [13] and core-polarization corrections due to Kuo and Osnes [14] and (ii) in a truncated model space allowing

at most one-particle excitations from the $f_{7/2}$ shell using an empirical interaction. In our tables we only cite the values corresponding to (i), as the spectroscopic factors are rather similar.

McGrory used a modification of the Kuo–Brown [13] matrix elements in his calculations where the eight matrix elements diagonal in $f_{7/2}^2$ were considered as free parameters in a fit to 29 excitation energies and seven ground-state binding energies with all four fp orbits included in the active space. This interaction was called KB1 in subsequent systematic analyses by Cole [11,12], who considered various modifications of the basic Kuo–Brown interaction by modifying the interaction centroids. In making comparisons with the work of Cole the values calculated with the interaction KB1 are given, as there are generally not significant differences, as far as spectroscopic factors are concerned, with the other modified versions.

2.2. *Spectroscopic factors for single neutron stripping*

In Table 1 the calculated values of $(2J_f + 1)S$ for the FPD6 interaction are given for final states in the Ca isotopes and in ^{44}Sc and ^{45}Sc, and compared with available experimental and theoretical values.

$^{41}Ca \rightarrow {}^{42}Ca$. For stripping to the ground state good agreement with experiment is found, but to the lowest $2^+(1)$, $4^+(1)$ and $6^+(1)$ states our values (summed over l) are too large by factors between 1.7 and 3.6. This is probably a reflection of the oversimplified description of the ^{41}Ca ground state in our model space, on the one hand, and mixing with core-excited states in ^{42}Ca, on the other. Several states for nuclei in the lower part of the fp shell are known to have significant admixtures of core-excited intruder states e.g. the 0^+ and 2^+ states in ^{42}Ca (see also Ref. [1]).

$^{42}Ca \rightarrow {}^{43}Ca$. Our calculated strengths correspond reasonably well with the measured values, and are also close to those of Olsen and Osnes [10].

$^{43}Ca \rightarrow {}^{44}Ca$. Good agreement between theory and experiment is found for transitions to the $0^+(1)$, $4^+(2)$ and $6^+(1)$ states. Our $l = 3$ values are too high for the $2^+(1)$ and $4^+(1)$ transitions, but still smaller than the KB1 values of McGrory. The calculated values for $0^+(1)$ and $4^+(2)$ are also significantly closer to experiment than the KB1 values.

$^{44}Ca \rightarrow {}^{45}Ca$. Our calculated values to the $\frac{7}{2}^-$ ground state and the $\frac{3}{2}^-(2)$ state lie within the rather large experimental limits shown. For the $\frac{3}{2}^-(1)$ transition our calculated value is too small by a factor of 3, but better than KB1. The $\frac{1}{2}^-(1)$ value is smaller than KB1 by about a factor of two, but is much closer to experiment, while KB1 is somewhat closer to the experimental value than our value for the transition to $\frac{3}{2}^-(3)$.

Table 1
Experimental and calculated spectroscopic factors for neutron stripping to states of various nuclei. The values of $(2J_f+1)S$ are shown, and final states are labelled by their spin $J(i)$, where i indicates the ith theoretical state of that spin, and the experimental and theoretical excitation energies E_x^{exp} and E_x^{th} are in MeV. (Energy levels marked with ◇ indicate levels where the experimental counterpart is not clearly established.) States marked with an asterisk were not used in the original fits to obtain the FPD6 interaction. Experimental spectroscopic factors are all from Ref. [4] unless otherwise stated. Other theoretical spectroscopic factors from the literature are indicated by Lit.

			Calculated				Exp. [4]		Lit.	
$J(i)$	E_x^{exp}	E_x^{th}	$f_{7/2}$	$p_{3/2}$	$\sum_{l=3}$	$\sum_{l=1}$	$\sum_{l=3}$	$\sum_{l=1}$	$\sum_{l=3}$	$\sum_{l=1}$
$^{41}Ca \rightarrow {}^{42}Ca$										
0(1)	0.000	0.000	1.81		1.81		1.6 ± 0.2			
2(1)	1.525	1.781	8.63	0.55	8.63	0.55	2.4 ± 0.6	0.2 ± 0.1		
4(1)	2.752	2.709	16.68	0.48	16.72	0.58	7.7 ± 2.0	0.27 ± 0.09		
6(1)	3.189	3.145	25.70		25.85		15.6 ± 3.9			
$^{42}Ca \rightarrow {}^{43}Ca$									Ref. [10]	
$\frac{7}{2}(1)$	0.000	0.000	6.00		6.00		4.64 ± 0.48		6.00	
$\frac{5}{2}(1)$	0.373	0.516			0.05		< 0.12		0.05	
$\frac{3}{2}(1)$	0.593	0.909		0.05		0.05		0.16 ± 0.08		0.02
$\frac{3}{2}(2)$	2.046	2.019		3.71		3.71		2.9±0.4		3.69
$^{43}Ca \rightarrow {}^{44}Ca$									Ref. [15]	
0(1)	0.000	0.000	3.64		3.64		3.1 ± 0.3		4.0	
2(1)	1.157	1.619	5.63	0.57	5.67	0.57	2.05 ± 0.55	0.40 ± 0.10	6.4	
4(1)	2.283	2.552	4.65	0.06	4.84	0.11	1.26 ± 0.36	0.09 ± 0.09	8.0	
*4(2)	3.044	2.939	6.75	0.01	6.76	0.06	8.2±2.1		4.0	
6(1)	3.285	3.187	17.31		17.32		20.0 [16]		17.6	
$^{43}Sc \rightarrow {}^{44}Sc$										
2(1)	0.000	0.000	3.69	0.00	3.91	0.00				
6(1)	0.271	0.651	14.21		14.22					
4(1)	0.350	0.529	7.52	0.38	7.58	0.39				
1(1)	0.667	1.242	1.07		1.26					
3(1)	0.763	0.807	0.14	0.19	0.24	0.23				
7(1)	0.947	1.231	5.75		5.75					
5(1)	1.052	1.156	0.62	0.08	0.71	0.08				
$^{44}Ca \rightarrow {}^{45}Ca$									Ref. [12]	
$\frac{7}{2}(1)$	0.000	0.000	4.03		4.03		2.9 ± 2.9 [6]		4.03	
$\frac{5}{2}(1)$	0.174	0.446			0.02				0.01	
$\frac{3}{2}(1)$	1.435	1.522		0.13		0.13		0.40 ± 0.04 [6]		0.01
$*\frac{3}{2}(2)$	1.900	1.889		3.39		3.39		2.2 ± 2.2 [6]		3.44
$\frac{1}{2}(1)$	2.249	2.914				0.24		0.30 ± 0.03 [6]		0.46
$*\frac{3}{2}(3)$	2.842	3.201		0.19		0.19		0.34 ± 0.04 [6]		0.26

Table 1 — continued

			Calculated				Exp. [4]		Lit.	
$J(i)$	E_x^{exp}	E_x^{th}	$f_{7/2}$	$p_{3/2}$	$\sum_{l=3}$	$\sum_{l=1}$	$\sum_{l=3}$	$\sum_{l=1}$	$\sum_{l=3}$	$\sum_{l=1}$
$^{44}Sc \rightarrow {}^{45}Sc$										
$*\frac{7}{2}(1)$	0.000	0.000	2.78	0.00	2.81	0.00				
$*\frac{3}{2}(1)$	0.376	0.666	0.15	0.19	0.18	0.20				
$*\frac{11}{2}(1)$	1.236	1.344	2.23		2.23					
$*\frac{1}{2}(1)$	1.555	1.381		0.00	0.00	0.11				
$*\frac{9}{2}(1)$	1.662	2.376	0.70		0.71					
$*\frac{5}{2}(1)$	2.092	1.575	4.69	0.03	4.69	0.04				
$*\frac{3}{2}(2)$	2.341	2.314	1.57	0.26	1.64	0.26				
$*\frac{9}{2}(2)$	◇	2.590	2.00		2.00					
$*\frac{11}{2}(2)$	◇	2.592	5.41		5.41					
$^{45}Ca \rightarrow {}^{46}Ca$										
0(1)	0.000	0.000	5.48		5.48					
2(1)	1.346	1.576	2.89	0.37	2.96	0.37				
4(1)	2.574	2.757	5.93	0.00	5.97	0.01				
6(1)	2.973	3.119	8.73		8.73					
$^{46}Ca \rightarrow {}^{47}Ca$									Ref. [12]	
$*\frac{7}{2}(1)$	0.000	0.000	2.05		2.05		2.1 [7]		2.1	
$*\frac{1}{2}(1)$	2.849	2.675				0.26		0.10 [7]		0.45
$*\frac{3}{2}(1)$	2.013	1.644		3.39		3.39		3.9 [7]		3.2
$*\frac{5}{2}(1)$	◇	3.225			0.02				0.01	
$^{47}Ca \rightarrow {}^{48}Ca$										
0(1)	0.000	0.000	7.38		7.38					
2(1)	3.832	3.659	0.11	4.61	0.18	4.61				
*3(1)	4.612	4.362	0.07	6.14	0.07	6.36				
*4(1)	4.504	4.134	0.01	8.09	0.12	8.11				
$^{48}Ca \rightarrow {}^{49}Ca$									Ref. [12]	
$\frac{3}{2}(1)$	0.000	0.000		3.67		3.67		3.4 [8]		3.52
$*\frac{1}{2}(1)$	2.022	2.367				1.88		2.16 [8]		1.86

$^{46}Ca \rightarrow {}^{47}Ca$. The values for $\frac{7}{2}^-(1)$ and $\frac{3}{2}^-(1)$ agree well with experiment, while that for $\frac{1}{2}^-(1)$ is about two-and-a-half times too large, but closer to experiment compared to the value of KB1.

$^{48}Ca \rightarrow {}^{49}Ca$. Good agreement is obtained with the two measured experimental values; our values are close to those of KB1.

Table 2
Experimental and calculated $(2J_f + 1)S$ values for proton stripping to states of various nuclei. Conventions are the same as used in Table 1

			Calculated				Exp. [4]		Lit.	
$J(i)$	E_x^{exp}	E_x^{th}	$f_{7/2}$	$p_{3/2}$	$\sum_{l=3}$	$\sum_{l=1}$	$\sum_{l=3}$	$\sum_{l=1}$	$\sum_{l=3}$	$\sum_{l=1}$
$^{42}Ca \rightarrow {}^{43}Sc$									Ref. [10]	
$\frac{7}{2}(1)$	0.000	0.000	6.55		6.55		6.48±0.96		4.22	
$\frac{3}{2}(1)$	0.980 [a]	0.876		1.55		1.55	1.48 [b]		1.06	
$^{43}Ca \rightarrow {}^{44}Sc$									Ref. [15]	
2(1)	0.000	0.000	2.57	0.00	2.75	0.00	3.00 ± 0.75		3.2	0.0
6(1)	0.271	0.651	7.66		7.74		8.19 ± 1.69		7.5	
4(1)	0.350	0.529	4.54	0.20	4.67	0.24	5.13 ± 1.08	0.27±0.09	5.3	0.0
1(1)	0.667	1.242	1.29		1.32		1.59 ± 0.42		2.1	
3(1)	0.763	0.807	0.22	0.60	0.22	0.83	1.75 ± 0.49	0.56±0.14	2.1	0.0
7(1)	0.947	1.231	16.27		16.27		17 [16]		17.1	
5(1)	1.052	1.156	1.34	2.10	1.35	2.10	3.6 [16]	1.7 [16]	4.3	1.1
*5(2)	1.532	1.797	9.09	0.16	9.09	0.16	8.0 [16]	0.4 [16]	5.3	0.0
*3(2)	◇	1.678	5.27	0.00	5.27	0.05			4.3	0.0
*4(2)	◇	2.220	1.49	0.70	1.49	0.90			1.1	0.0
*4(3)	◇	2.602	0.04	1.99	0.04	1.99			0.0	2.1
*6(2)	◇	2.678	1.56		1.64				2.1	
*5(3)	◇	3.126	0.35	0.53	0.84	0.53			1.1	0.0
$^{44}Ca \rightarrow {}^{45}Sc$									Ref. [12]	
$*\frac{7}{2}(1)$	0.000	0.000	5.93		5.93		(7.10) [6]		6.25	
$*\frac{3}{2}(1)$	1.067	0.666		1.13		1.13				0.55
$*\frac{1}{2}(1)$	1.555	1.381				0.19		0.35 [6]		0.11
$*\frac{5}{2}(1)$	2.092	1.575			0.23				0.10	
$*\frac{3}{2}(2)$	2.341	2.314		0.00		0.00		(0.15) [6]		0.01

[a] An average value for the two experimental levels at 0.473 and 1.179 MeV, weighted by the experimental single-nucleon strength.
[b] The sum of the strengths to the two lowest $\frac{3}{2}$ states.

2.3. *Spectroscopic factors for single proton stripping*

In Table 2 the calculated values of $(2J_f+1)S$ for single proton stripping are displayed. The same conventions as with the spectroscopic factors for single neutron stripping applies.

$^{42}Ca \rightarrow {}^{43}Sc$. Excellent agreement for the transitions to the $\frac{7}{2}^-(1)$ ground state and the $\frac{3}{2}^-(1)$ state (using the sum of the fragmented experimental strengths for the two lowest $\frac{3}{2}^-$ states) is obtained; both values of KB1 are significantly lower.

$^{43}Ca \rightarrow {}^{44}Sc$. Good general agreement with experiment is obtained – most of our calculated values lie within the experimental limits. The $l = 3$ contribution to $\frac{3}{2}^-(1)$

Table 3
Experimental and calculated spectroscopic factors S for proton pickup to states of ^{44}Ca. Conventions are the same as used in Table 1

			Calculated				Exp. [4]		Lit.	
$J(i)$	E_x^{exp}	E_x^{th}	$f_{7/2}$	$p_{3/2}$	$\sum_{l=3}$	$\sum_{l=1}$	$\sum_{l=3}$	$\sum_{l=1}$	$\sum_{l=3}$	$\sum_{l=1}$
^{45}Sc → ^{44}Ca									Ref. [12]	
0(1)	0.000	0.000	0.74		0.74		0.50 ± 0.13		0.78	
2(1)	1.157	1.619	0.23	0.08	0.24	0.08	0.18 ± 0.03		0.27	0.04
4(1)	2.283	2.552	0.05	0.01	0.06	0.02	0.09 ± 0.03		0.05	0.02
6(1)	3.285	3.187	0.00		0.00				0.00	0.00

is evidently much too small (KB1 is much closer), but the $l = 1$ contribution agrees reasonably well, while KB1 gives no strength for this branch. Also the $l = 3$ contribution to $\frac{5}{2}^-(1)$ is too small, with KB1 being closer. The relatively large strength to $\frac{5}{2}^-(2)$ is well reproduced, and is significantly better than KB1. Also the large strength to $\frac{7}{2}^-(1)$ is accurately reproduced by both FPD6 and KB1.

$^{44}Ca \rightarrow {}^{45}Sc$. For stripping to the $\frac{7}{2}^-(1)$ ground state a good correspondence with experiment is found; in the case of the $\frac{1}{2}^-(1)$ transition the FPD6 value is too small by roughly a factor of two, whereas the KB1 value is even less. For the $\frac{3}{2}^-(2)$ transition the very weak strength observed supports the predictions of FPD6 and KB1.

2.4. *Spectroscopic factors for single proton pickup*

In Table 3 the presently calculated single proton pickup spectroscopic factors to ^{44}Ca are compared with experimental values. For pickup to the ground state our calculated value is about 50% too high, whereas the remaining observed values are reproduced much better. The FPD6 values are quite close to those of KB1.

2.5. *Spectroscopic factors for single neutron pickup*

In Table 4 the calculated spectroscopic factors for single neutron pickup are compared.

$^{43}Ca \rightarrow {}^{42}Ca$. The spectroscopic factor to the 0^+ ground state is reasonably well reproduced although it lies outside the experimental limits indicated. For the much weaker $2^+(1)$ transition our value is about a factor of two too large. The remaining two experimental values are well reproduced. Our values are very close to the calculated ones of Ref. [9], in which McGrory et al. used a slightly modified version of the Kuo–Brown interaction (KB1).

$^{44}Ca \rightarrow {}^{43}Ca$. The ground-state value is slightly higher than experiment and close to McGrory's calculated value [15]. For the $\frac{5}{2}^-(1)$ state our value is too small while that

Table 4
Experimental and calculated spectroscopic factors S for neutron pickup to states of various nuclei. Conventions are the same as used in Table 1

			Calculated				Exp. [4]		Lit.	
$J(i)$	E_x^{exp}	E_x^{th}	$f_{7/2}$	$p_{3/2}$	$\sum_{l=3}$	$\sum_{l=1}$	$\sum_{l=3}$	$\sum_{l=1}$	$\sum_{l=3}$	$\sum_{l=1}$
$^{43}Ca \rightarrow ^{42}Ca$									Ref. [9]	
0(1)	0.000	0.000	0.75		0.75		0.58 ± 0.06		0.75	
2(1)	1.525	1.781	0.34	0.00	0.35	0.00	0.18 ± 0.03		0.37	
4(1)	2.752	2.709	0.68	0.00	0.68	0.00	0.59 ± 0.10	(0.01)	0.68	
6(1)	3.189	3.145	0.99		0.99		0.99 ± 0.18		0.99	
$^{44}Ca \rightarrow ^{43}Ca$									Ref. [15]	
$\frac{7}{2}(1)$	0.000	0.000	3.64		3.64		3.1 ± 0.3		3.6	
$\frac{5}{2}(1)$	0.373	0.516			0.03		0.17 ± 0.08		0.1	
$\frac{3}{2}(1)$	0.593	0.909		0.02		0.02		0.10 ± 0.03		0.0
$\frac{3}{2}(2)$	2.046	2.019		0.14		0.14		0.19 ± 0.06		0.1
$^{44}Sc \rightarrow ^{43}Sc$										
$\frac{7}{2}(1)$	0.000	0.000	0.74	0.00	0.78	0.00				
$\frac{3}{2}(1)$	0.980 [a]	0.876	0.01	0.02	0.01	0.02				
$\frac{11}{2}(1)$	1.830	1.871	0.43		0.43					
$\frac{9}{2}(1)$	2.459	2.601	0.45		0.46					
$^{45}Ca \rightarrow ^{44}Ca$										
0(1)	0.000	0.000	0.50		0.50					
2(1)	1.157	1.619	0.70	0.00	0.70	0.00				
4(1)	2.283	2.552	0.59	0.00	0.60	0.00				
*4(2)	3.044	2.939	0.78	0.00	0.79	0.00				
6(1)	3.285	3.187	1.98		1.98					
$^{45}Sc \rightarrow ^{44}Sc$									Ref. [12]	
2(1)	0.000	0.000	0.35	0.00	0.35	0.00	0.34 ± 0.05		0.36	
6(1)	0.271	0.651	0.39		0.43		0.49 ± 0.07		0.44	
4(1)	0.350	0.529	0.34	0.02	0.34	0.02	0.37 ± 0.05	0.03 ± 0.01	0.33	0.01
1(1)	0.667	1.242	0.29		0.30		0.33 ± 0.05		0.32	
3(1)	0.763	0.807	0.03	0.00	0.04	0.00	0.19 ± 0.03	small	0.14	0.00
7(1)	0.947	1.231	1.09		1.09		1.3 [16]		1.18	
5(1)	1.052	1.156	0.14	0.04	0.15	0.04	0.25 [16]	0.04 [16]	0.18	0.02
*5(2)	1.532	1.797	0.19	0.03	0.19	0.03			0.12	0.03
*3(2)	◇	1.678	0.23	0.02	0.23	0.02			0.14	0.01
$^{46}Ca \rightarrow ^{45}Ca$									Ref. [12]	
$\frac{7}{2}(1)$	0.000	0.000	5.48		5.48		6.0 [6] 6.5 ± 1.5 [6]		5.39	
$\frac{5}{2}(1)$	0.174	0.446			0.03		< 0.12 [6] < 0.25 [6]		0.02	
$\frac{3}{2}(1)$	1.435	1.522				0.04		0.15 [6]		0.01
$*\frac{3}{2}(2)$	1.900	1.889		0.12		0.12		< 0.08 [6] < 0.04 [6]		0.16
$\frac{1}{2}(1)$	2.249	2.914				0.00				0.01
$*(\frac{3}{2})(3)$	2.842	3.201		0.02		0.02		0.15 [6]		0.03

Table 4 — continued

			Calculated				Exp. [4]		Lit.	
$J(i)$	E_x^{exp}	E_x^{th}	$f_{7/2}$	$p_{3/2}$	$\sum_{l=3}$	$\sum_{l=1}$	$\sum_{l=3}$	$\sum_{l=1}$	$\sum_{l=3}$	$\sum_{l=1}$
$^{47}Ca \rightarrow ^{46}Ca$										
0(1)	0.000	0.000	0.26		0.26					
2(1)	1.346	1.576	1.13	0.01	1.13	0.01				
4(1)	2.574	2.757	2.05	0.01	2.05	0.01				
6(1)	2.973	3.119	2.99		3.00					
$^{48}Ca \rightarrow ^{47}Ca$									Ref. [12]	
$*\frac{7}{2}(1)$	0.000	0.000	7.38		7.38		6.7±1.4 [7]		7.10	
$*\frac{1}{2}(1)$	2.849	2.675				0.00				0.00
$*\frac{3}{2}(1)$	2.013	1.644		0.08		0.08		0.02±0.01 [7]		0.17
$*\frac{5}{2}(1)$	◇	3.225			0.01				0.01	

[a] An average value for the two experimental levels at 0.473 and 1.179 MeV, weighted by the experimental single-nucleon strength.

of McGrory does better. For the $\frac{3}{2}^-(1)$ transition both theoretical values are too small and for $\frac{3}{2}^-(2)$ our value lies closer to experiment than McGrory's.

$^{45}Sc \rightarrow ^{44}Sc$. Very close agreement with experiment is found for the $l = 3$ and 1 components for pickup to almost all the states listed. The $l = 3$ value to $\frac{3}{2}^-(1)$ is too small, whereas KB1 does better. Most of our calculated values are quite close to KB1, except for the case just mentioned and the $l = 3$ values to $\frac{3}{2}^-(2)$ and $\frac{5}{2}^-(2)$.

$^{46}Ca \rightarrow ^{45}Ca$. Our values are close to KB1 and fair agreement is found between theory and experiment for the transition to the ground state. The strengths to the three $\frac{3}{2}^-$ states are predicted to be relatively weak, but somewhat different from the experimental ones.

$^{48}Ca \rightarrow ^{47}Ca$. The ground-state spectroscopic factor lies within the experimental limits and the remaining strengths are calculated to be quite small. In the case of the $\frac{3}{2}^-(1)$ transition our value is better than KB1.

2.6. Summary

It has been shown that the wave functions based on the FPD6 interaction reproduce the spectroscopic factors for nuclei up to mass 49 quite well in general. In cases where our calculations differ significantly from calculations with other interactions, particularly for the weaker transitions, the FPD6 values in most cases agree better with experiment. This suggests that FPD6 gives a more reliable description of the wave functions of the states involved. The values for the FPMI3 interaction are very close to those of FPD6, differing in most cases by only one or two per cent.

3. Electromagnetic properties of $A = 41$–49 nuclei

In this section the wave functions obtained with the FPD6 interaction are used to calculate electromagnetic properties. Effective operators were used to account for the configurations that were excluded by our model space. The renormalization of the electromagnetic multipole operators is usually expressed in terms of effective charges and g-factors. These may either be calculated microscopically [14] or determined empirically by fitting the experimental data.

3.1. Magnetic dipole and electric quadrupole moments

These have been calculated in Ref. [1] for the FPD6 and FPMI3 interactions using effective nucleon g-factors and charges determined from least-squares fits. However, it appears that the magnetic moment data in the lower part of the fp shell is insufficient to determine both the spin and orbital g-factors accurately. We therefore recalculate the magnetic dipole moments by fixing the orbital g-factors at the bare values, $g_l(\mathrm{IS}) = 0.5$ and $g_l(IV) = 0.5$, and varying the spin g-factors. The values adopted for FPD6 are $g_s(\mathrm{IS}) = 1.15$ and $g_s(\mathrm{IV}) = 4.34$ and for FPMI3 $g_s(\mathrm{IS}) = 1.19$, $g_s(\mathrm{IV}) = 4.38$. (The bare values for the spin g-factors are $g_s(\mathrm{IS}) = 0.88$ and $g_s(\mathrm{IV}) = 4.706$.) It is evident that the fitted values for the two interactions are very close to each other.

The calculated values for the ground-state magnetic dipole moments for the nuclei in the lower part of the fp shell have been plotted against experimental values in Fig. 1. The experimental values are plotted along the vertical axis and the theoretical values

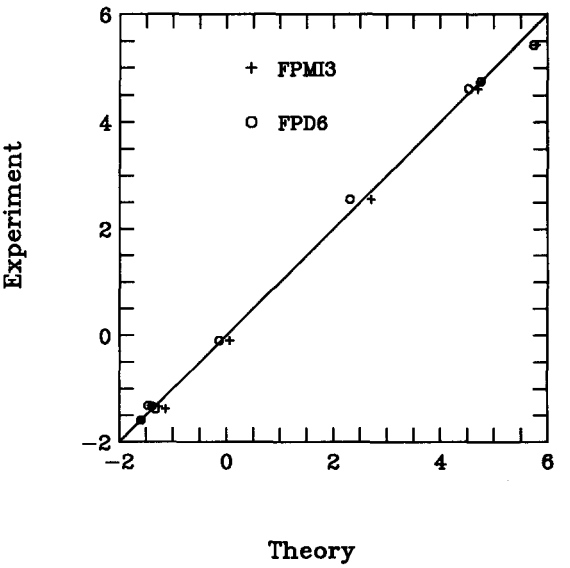

Fig. 1. Comparison of experimental and theoretical magnetic dipole moments in units of μ_N^2. The effective g-factors are $g_l(\mathrm{IS}) = 0.5$, $g_l(\mathrm{IV}) = 0.5$, with $g_s(\mathrm{IS}) = 1.15$ and $g_s(\mathrm{IV}) = 4.34$ for FPD6, and $g_s(\mathrm{IS}) = 1.19$ and $g_s(\mathrm{IV}) = 4.38$ for FPMI3.

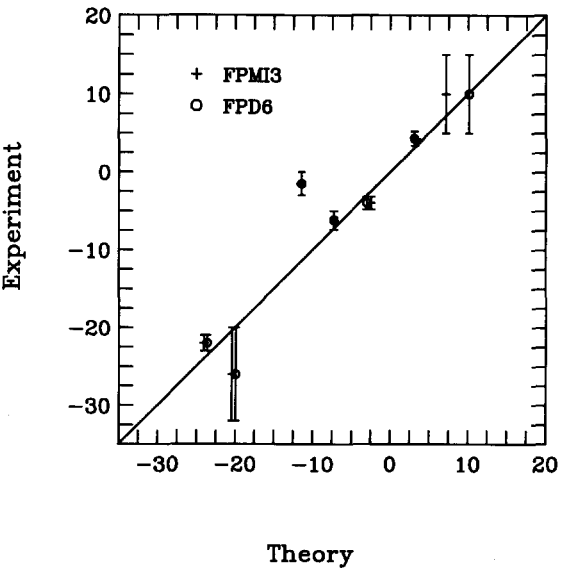

Fig. 2. Comparison of experimental and theoretical electric quadrupole moments in units of e^2fm^4. The effective charges are $e_p = 1.33$, $e_n = 0.64$.

obtained with the effective nucleon g-factors for both the FPD6 (circles) and FPMI3 (pluses) are plotted along the horizontal axis. The 45° line signifies agreement with experiment. It is evident that good agreement with experiment is obtained and that there is little difference between the results for both our interactions. For completeness, and to stress the similarity in results for the two interactions, the electric quadrupole moments of Ref. [1] are also plotted in Fig. 2 ($e_p = 1.33$ and $e_n = 0.64$).

3.2. *Electromagnetic transition rates*

3.2.1. *Comparison with experiment*

The wave functions of the FPD6 interaction have been used to calculate the $B(E2)$ and $B(M1)$ values for transitions in the $A = 41$–49 mass range. The experimental and calculated M1 and E2 transition rates are compared in Table 5. There are about ten transitions that apparently involve inadequate wave functions, whose strengths cannot be significantly improved in a consistent way by using effective charges (they are marked by asterisks in Table 5). If these are omitted and a least-squares fit of the $B(E2)$ values to experiment is carried out, values of $e_p = 1.35$ and $e_n = 0.67$ are obtained, which is consistent with those we found for the static E2 moments ($e_p = 1.33$ and $e_n = 0.64$) in Ref. [1]. Hence we have also used the latter values to calculate the $B(E2)$'s in the present work, and the $B(M1)$'s were calculated using the effective g-factors found above. These values for the effective charges are larger than those used by McGrory [15] ($e_p = 1.2e$ and $e_n = 0.5e$), but are close to those used in the projected Hartree–Fock calculations in this mass region [17]. The values of McGrory were used

Table 5
B(E2) and B(M1) transition rates in low-lying fp-shell nuclei (using the FPD6 interaction with Δe_p = 0.33, Δe_n = 0.64 and g_s(IS) = 1.15, g_s(IV) = 4.34, g_l(IS) = 0.50, g_l(IV) = 0.50). Experimental excitation energies E_x are in MeV

Nuclide	Transition [a]			B(E2) values (e^2fm^4)		B(M1) values (μ_N^2)	
	$J_i^\pi(E_{x_i})$	→	$J_f^\pi(E_{x_f})$	experiment	calculation	experiment	calculation
^{42}Ca [b]	$^*2^+(1.52)$	→	$0^+(0)$	81.5 ± 3.0	13.35	–	–
	$^*4^+(2.75)$	→	$2^+(1.52)$	57.5 ± 4.5	13.87	–	–
	$6^+(3.19)$	→	$4^+(2.75)$	6.44 ± 0.19	7.387	–	–
^{42}Sc [c]	$1^+,0(0.61)$	→	$0^+,1\,(0)$	–	–	3.6 ± 1.4	6.25
	$3^+,0(1.49)$	→	$1^+,0(0.61)$	35 ± 6 34.4 ± 6.3	41.76	–	–
	$5^+,0(1.51)$	→	$7^+,0(0.62)$	20 ± 3 $25.1^{+5.4}_{-3.8}$	40.02	–	–
		→	$3^+,0(1.49)$	–	45.61	–	–
^{43}Ca [d]	$\frac{5}{2}^-(0.37)$	→	$\frac{7}{2}^-(0)$	86 ± 7	30.56	$(2.3 \pm 0.2) \times 10^{-2}$	1.23×10^{-2}
	$^*\frac{3}{2}^-(0.59)$	→	$\frac{7}{2}^-(0)$	65.5 ± 4.5	16.51	–	–
		→	$\frac{5}{2}^-(0.37)$	–	33.41	$(1.36 \pm 0.11) \times 10^{-2}$	0.93×10^{-2}
	$\frac{11}{2}^-(1.68)$	→	$\frac{7}{2}^-(0)$	55 ± 16	15.12	–	–
	$\frac{15}{2}^-(2.75)$	→	$\frac{11}{2}^-(1.68)$	16.6 ± 0.7	12.49	–	–
^{43}Sc [d]	$^*\frac{3}{2}^-(0.47)$	→	$\frac{7}{2}^-(0)$	143 ± 9	128.3	–	–
	$^*\frac{3}{2}^-(1.18)$	→	$\frac{7}{2}^-(0)$	81 ± 27		–	–
	$^*\frac{11}{2}^-(1.83)$	→	$\frac{7}{2}^-(0)$	123^{+22}_{-16}	46.79	–	–
	$\frac{9}{2}^-(2.46)$	→	$\frac{7}{2}^-(0)$	–	12.43		0.419
		→	$\frac{11}{2}^-(1.83)$	–	16.49	–	1.02
^{43} Sc [d]	$\frac{15}{2}^-(2.99)$	→	$\frac{11}{2}^-(1.83)$	49^{+8}_{-6}	49.54	–	–
	$\frac{19}{2}^-(3.12)$	→	$\frac{15}{2}^-(2.99)$	27.0 ± 0.8	30.43	–	–
^{44}Ca [b]	$^*2^+(1.16)$	→	$0^+(0)$	100 ± 6	22.90	–	–
	$^*4^+(2.28)$	→	$2^+(1.16)$	75 ± 15 160 ± 60	18.98	–	–
	$^*6^+(3.28)$	→	$4^+(2.28)$	41.2 ± 3.6 50 ± 12	8.774	–	–
^{44}Sc [e]	$4^+(0.35)$	→	$2^+(0)$	33.2 ± 1.8	42.53	–	–
	$1^+(0.67)$	→	$2^+(0)$	–	49.99	2.68 ± 1.07	6.88
^{44}Ti [e]	$2^+(1.08)$	→	$0^+(0)$	129 ± 28	135.4	–	–
	$4^+(2.45)$	→	$2^+(1.08)$	277 ± 46	184.4	–	–
	$6^+(4.02)$	→	$4^+(2.45)$	148 ± 18	155.9	–	–

Table 5 — continued

Nuclide	Transition [a]			B(E2) values (e^2fm^4)		B(M1) values (μ_N^2)	
	$J_i^\pi(E_{x_i})$	→	$J_f^\pi(E_{x_f})$	experiment	calculation	experiment	calculation
^{45}Ca [f]	$\frac{5}{2}^-(0.17)$	→	$\frac{7}{2}^-(0)$	–	41.70	$(1.86 \pm 0.20) \times 10^{-2}$	0.80×10^{-2}
	$\frac{3}{2}^-(1.43)$	→	$\frac{7}{2}^-(0)$	$\geqslant 1.8 \times 10^{-3}$	14.91	–	–
		→	$\frac{5}{2}^-(0.17)$	$\geqslant 4.7 \times 10^{-4}$	0.549	$\geqslant 1.6 \times 10^{-7}$	9.6×10^{-3}
^{45}Sc [g]	$\frac{11}{2}^-(1.24)$	→	$\frac{7}{2}^-(0)$	85 ± 8	64.29	–	–
	$\frac{15}{2}^-(2.11)$	→	$\frac{11}{2}^-(1.24)$	< 85	56.4	–	–
	$*\frac{9}{2}^-(1.66)$	→	$\frac{7}{2}^-(0)$	72 ± 6	7.500	0.04 ± 0.01	0.053
		→	$\frac{11}{2}^-(1.24)$	< 400	9.565	0.60 ± 0.15	0.392
^{45}Ti [f]	$\frac{3}{2}^-(0.037)$	→	$\frac{7}{2}^-(0)$	155 ± 11	161.5	–	–
	$\frac{5}{2}^-(0.04)$	→	$\frac{7}{2}^-(0)$	$< 3.7 \times 10^5$	209.8	$(4.17 \pm 0.18) \times 10^{-2}$	8.3×10^{-2}
	$\frac{9}{2}^-(1.35)$	→	$\frac{5}{2}^-(0.04)$	103 ± 16	135.5	–	–
		→	$\frac{7}{2}^-(0)$	145 ± 66	104.2	0.124 ± 0.014	0.189
	$\frac{11}{2}^-(1.47)$	→	$\frac{7}{2}^-(0)$	171 ± 29	154.8	–	–
^{46}Ca [b]	$2^+(1.35)$	→	$0^+(0)$	35.1 ± 3.6	20.52	–	–
	$4^+(2.58)$	→	$2^+(1.35)$	–	13.69	–	–
	$6^+(2.97)$	→	$4^+(2.58)$	5.34 ± 0.28	5.948	–	–
^{47}Ca [h]	$\frac{3}{2}^-(2.01)$	→	$\frac{7}{2}^-(0)$	< 2.8	2.338	–	–
^{48}Ca [i]	$2^+(3.83)$	→	$0^+(0)$	19 ± 9	22.96	–	–
^{49}Ca	$\frac{1}{2}^-(2.02)$	→	$\frac{3}{2}^-(0)$	–	25.24	–	0.632

[a] All experimental excitation energies are given in MeV.
[b] All the experimental data for the given nuclide were taken from Ref. [19].
[c] All the experimental B(E2) data for the given nuclide were taken from Ref. [15] and B(M1) data from Ref. [20].
[d] All the experimental B(E2) data for the given nuclide were taken from Ref. [10], and the B(M1) data (where applicable) from Ref. [21].
[e] All the experimental data for the given nuclide were taken from Ref. [21].
[f] All the experimental data for the given nuclide were taken from Ref. [6].
[g] All the experimental data for the given nuclide were taken from Refs. [6,22].
[h] All the experimental data for the given nuclide were taken from Ref. [7].
[i] All the experimental data for the given nuclide were taken from Ref. [23].
* States with possible large intruder state admixture.

for the effective charges in the initial calculations of Cole [11] in the fp shell but in later calculations [18] the larger values ($e_p = 1.33e$ and $e_n = 0.64$) for the effective charges were used for the E2 rates. It was also shown by Cole [11,18] that the M1 transition rates calculated with effective operators which reproduce the M1 ground-state moments of ^{41}Ca and ^{41}Sc are only marginally better than those calculated with free-nucleon operators.

The experimental E2 and M1 transition rates tabulated in Table 5 were taken from

Refs. [6,7,10,15] and [19–23]. The excitation energies (in MeV) of the final and initial states are indicated in brackets.

The B(E2) values for transitions involving low-spin states in ^{42}Ca, ^{43}Ca, ^{43}Sc and ^{44}Ca are too low by factors of about 3–6 when compared to the experimental values. There are several low-lying intruder states in this mass region, particularly the 0^+(1.84 MeV) and 2^+(2.42 MeV) states in ^{42}Ca, the lowest $\frac{5}{2}^-$ (0.85 MeV) and second $\frac{7}{2}^-$ (1.41 MeV) states in ^{43}Sc, the 0^+(1.88 MeV) and 2^+(2.66 MeV) states in ^{44}Ca, and the 0^+ state at 2.42 MeV in ^{46}Ca. It can therefore be expected that a certain amount of mixing with such states can occur. In ^{42}Ca, for example, the $2^+ \rightarrow 0^+_{(g.s.)}$ and $4^+ \rightarrow 2^+$ transition rates imply a much larger effective charge than does the $6^+ \rightarrow 4^+$ transition, which indicates that the admixtures decrease significantly as one goes to higher-spin states. Better agreement is indeed achieved between the theoretical and experimental values for high-spin states assumed to consist of predominantly pure $(fp)^n$ configurations. For ^{42}Sc the agreement with experiment for the B(E2) values is also much better.

Apart from intruder admixtures, the wave functions for low-lying states in Ca isotopes have fairly pure $f^n_{7/2}$ configurations. M1 transitions between these states can only proceed through admixtures of $p_{3/2}$ and $f_{5/2}$ states since M1 transitions between identical particle states of pure $f^n_{7/2}$ configurations are forbidden [24]. These admixtures are small so that the theoretical M1 strengths are very weak. The values obtained for the two known M1 transitions in ^{43}Ca are in good agreement with experiment. This is a considerable improvement over values obtained with the Kuo–Brown interaction which are several orders of magnitude too small [15].

In ^{43}Sc there are two relatively strong B(M1) values predicted, for which there are no experimental values available. For the two strong transitions between the high-spin states in ^{43}Sc the B(E2) values are accurately reproduced, whereas the B(E2) value for the transition from the first $\frac{11}{2}^-$ state to the ground state is underpredicted by a factor of 2.6. In Ref. [1] we have considered the two lowest experimental $\frac{3}{2}^-$ states, weighted by the single-nucleon spectroscopic strength, as corresponding to the first $\frac{3}{2}^-$ shell-model state. We should therefore add the B(E2) values for the transitions from these two states to the ground state (224 e^2fm^4) when comparing with the shell-model value (128 e^2fm^4); however, the shell-model B(E2) value underpredicts the experimental value when this is done, as expected from the discussion of intruder admixtures above.

There are no strong M1 transitions predicted for ^{44}Ca because of angular-momentum selection rules and the pure-configuration inhibition mentioned above. For ^{44}Sc the strong E2 transition to the ground state is reasonably well reproduced, and the calculated B(M1) value to the ground state is within a factor 3 of the measured value.

Good agreement between the theoretical and experimental magnetic dipole transitions strengths in ^{45}Sc for the low-lying states is obtained. If the lowest $\frac{3}{2}^-$, $\frac{5}{2}^-$ and first excited $\frac{7}{2}^-$ states are assumed to be intruders, the B(E2) values involving other low-lying states correspond reasonably well with experiment, except for the transition from $\frac{9}{2}^-$ to the ground state, which is calculated too low by a factor 10.

Excellent agreement is obtained between the experimental and theoretical B(M1)

and $B(E2)$ values for the transitions in ^{45}Ti, bearing in mind that this nuclide was not included in the energy fits.

The theoretical $B(E2)$ values obtained for transitions in the $^{46-48}$Ca isotopes are in much better agreement with their experimental counterparts than those obtained for the $^{41-44}$Ca isotopes. No experimental data is available for ^{49}Ca, but the FPD6 interaction predicts a sizeable strength for the transition indicated.

3.2.2. Summary

It has been shown that the $B(E2)$ values obtained in the lower part of the shell for the low-spin states of ^{42}Ca, ^{43}Ca and ^{44}Ca are generally too low when compared with the experimental values, which implies that significant mixing with the low-lying intruder states occurring in this mass region takes place. For the high-spin states better agreement between calculated and experimental values is obtained. The agreement between calculated and experimental values for the Sc and Ti isotopes as well as ^{46}Ca–^{48}Ca is generally quite good. The measured $B(M1)$ values, with few exceptions, are also adequately reproduced by the FPD6 interaction.

For the FPMI3 interaction the transition strengths differ more from the FPD6 values than the spectroscopic factors, since the transition strengths are more sensitive to the details of the wave functions. For the $B(E2)$ values the differences are small, usually about 5–10%. For the $B(M1)$ strengths the two interactions also give quite similar results for the strong transitions, but for the weak transitions the FPD6 interaction does markedly better.

4. Gamow–Teller results

4.1. Gamow–Teller matrix elements

In Table 6 the theoretical values for the Gamow–Teller matrix elements obtained with the FPD6 interaction are compared to those obtained from experiment. The experimental values $B(GT)_{exp}$ were taken from Ref. [25] in which they were calculated from the expression for the observed partial half-life

$$t_{1/2} = \frac{C}{(f_v + f_{EC})B(F) + (f_a + f_{EC})B(GT)}, \tag{5}$$

with C a constant having the value (6170 ± 4) s as in Ref. [26], f_v and f_a the vector and axial vector phase-space factors which are calculated with formulae cited in Refs. [26,27] and f_{EC} the electron capture phase-space factor.

It is evident from Table 6 that the theoretical $B(GT)$ values determined with the free-nucleon g_A value are generally larger than the observed ones. One may define [25] an average renormalization factor by

$$\rho = \frac{1}{N}\sum_{i}^{N} \frac{B(GT;i)_{exp}^{1/2}}{B(GT;i)_{th}^{1/2\,free}}, \tag{6}$$

Table 6
A comparison between the theoretical and experimental Gamow–Teller matrix elements

Initial state (J^π)		Final state (J^π, E_x(MeV))		$B(\mathrm{GT})^{1/2}_{\mathrm{exp}}$	$B(\mathrm{GT})^{1/2\ \mathrm{free}}_{\mathrm{th}}$	$B(\mathrm{GT})^{1/2\ \mathrm{eff}}_{\mathrm{th}}$
^{41}Sc	$(\frac{7}{2}^-)$	^{41}Ca	$(\frac{7}{2}^-\ 0)$	1.072(9)	1.418	1.124
^{42}Sc	(7^+)	^{42}Ca	$(6^+\ 3.189)$	0.647(6)	0.840	0.666
^{42}Ti	(0^+)	^{42}Sc	$(1^+\ 0.611)$	1.99(4) [a]	2.751	2.182
			$(1^+\ 2.223)$	0.51(11) [a]	0.100	0.080
^{43}Sc	$(\frac{7}{2}^-)$	^{43}Ca	$(\frac{7}{2}^-\ 0)$	0.240(3)	0.305	0.249
			$(\frac{5}{2}^-\ 0.373)$	0.253(6)	0.182	0.144
^{43}Ti	$(\frac{7}{2}^-)$	^{43}Sc	$(\frac{7}{2}^-\ 0)$	0.907(14)	1.219	0.967
^{44}Sc	(2^+)	^{44}Ca	$(2^+\ 1.157)$	0.174(1)	0.187	0.150
^{45}Ca	$(\frac{7}{2}^-)$	^{45}Sc	$(\frac{7}{2}^-\ 0)$	0.079(1)	0.089	0.071
^{45}Ti	$(\frac{7}{2}^-)$	^{45}Sc	$(\frac{7}{2}^-\ 0)$	0.394(4)	0.513	0.407

[a] The branching ratio error is less than given in Table 42.19 of Ref. [28], because we use the $0^+ \rightarrow 0^+$ Fermi transition to calibrate the observed branching ratio.

$B(\mathrm{GT})^{1/2}_{\mathrm{exp}}$ denotes the experimental Gamow–Teller matrix elements determined from Eq. (5).

$B(\mathrm{GT})^{1/2\ \mathrm{free}}_{\mathrm{th}}$ are the theoretical Gamow–Teller matrix elements based on the free-nucleon single-particle Gamow–Teller matrix element.

$B(\mathrm{GT})^{1/2\ \mathrm{eff}}_{\mathrm{th}}$ are the theoretical Gamow–Teller matrix elements obtained by multiplying $B(\mathrm{GT})^{1/2\ \mathrm{free}}_{\mathrm{th}}$ with $\rho = 0.793$ determined from Eq. (7.2).

The experimental data were taken from Ref. [25].

where N is the total number of transitions, $B(\mathrm{GT})^{1/2}_{\mathrm{exp}}$ denotes the experimental Gamow–Teller matrix elements determined from Eq. (5) and $B(\mathrm{GT})^{1/2\ \mathrm{free}}_{\mathrm{th}}$ denotes the theoretical Gamow–Teller matrix elements based on the free-nucleon single-particle Gamow–Teller matrix elements.

Our results give $\rho = 0.793$ for the lower part of the fp shell, if the transitions to the 2.223 and 0.373 MeV excited states in ^{42}Sc and ^{43}Ca are excluded. This should be compared with the value of 0.748 for the $N_{\mathrm{jump}} = 2$ model of Miyatake et al. [25] in which at most two particles were allowed to be excited from the $0f_{7/2}$ orbit to the $1p_{3/2}$, $0f_{5/2}$ and $1p_{1/2}$ orbits. (The corresponding values obtained for the 0p shell [27] and 1s0d shell [29], respectively are 0.897 ± 0.034 and 0.76 ± 0.03.) If the free-nucleon values of $B(\mathrm{GT})^{1/2}$ are multiplied by 0.793 the values obtained (last column of Table 6) agree very well with experiment, with the exception of the two transitions referred to above. The corresponding FPMI3 values are fairly close to the FPD6 values.

5. Gamow–Teller strength distributions

The theoretical Gamow–Teller transition strength distributions, determined with the fp shell wave functions obtained with the FPD6 interaction, have been calculated for the nuclei in the mass range of interest, and are available from the authors. It was shown in Ref. [31] that the MSOBEP interaction form gives good agreement for the Gamow–

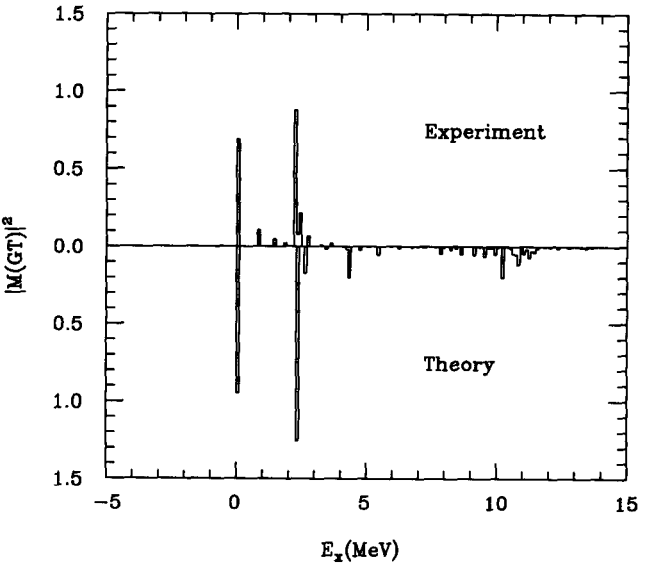

Fig. 3. Comparison of experimental and theoretical (free-nucleon) Gamow–Teller strength distributions for ^{43}Ti $\rightarrow$ ^{43}Sc. The excitation energy is in MeV. The two largest peaks correspond to the $\frac{7}{2}^-$ ground state and the $\frac{5}{2}^-$ state at 2.29 MeV experimental excitation energy.

Teller distribution in $A = 48$. For the ^{43}Ti $\rightarrow$ ^{43}Sc transitions the experimental distribution has also been measured up to 5 MeV excitation energy [30], and a comparison with our calculation is given in Fig. 3. The free-nucleon strengths are plotted as a function of the theoretical excitation energy in the final nucleus. Note that we use the definition $B(\mathrm{GT}) = (g_\mathrm{A}/g_\mathrm{V})^2 M(\mathrm{GT})^2$.

Most of the Gamow–Teller strength is concentrated in the transitions to the lowest levels of each spin [30]. It is interesting that in the theoretical case the Gamow–Teller strength distribution extends up to about 14 MeV excitation in ^{43}Sc. The total observed Gamow–Teller strength $\sum |M(\mathrm{GT})|^2 = 1.35 \pm 0.15$ [30] whereas a value of about 2.65 up to 5 MeV excitation is predicted by the FPD6 interaction, giving a quenching factor of 0.51. This once again illustrates the quenching phenomena for the Gamow–Teller strengths.

6. Summary and conclusion

A study of the lower fp shell nuclei ($A = 41$–49) in the full fp configuration space has been carried out. It was demonstrated in Ref. [1] that the same basic semi-empirical interaction form MSOBEP that was applied successfully in the 1s0d shell, with far fewer parameters than purely empirical interactions, yielded good fits to energy data in the 0f1p shell. The final interaction, denoted by FPD6, containing only 10 variable parameters, was obtained by fitting to a set of level energies in the lower part of the fp shell. A fit of two-body matrix elements using the linear combination method gave comparable

results with 12 parameters varied, and this interaction was denoted by FPMI3. Generally good agreement with experimental level energies and static electromagnetic moments has been obtained with the wave functions calculated from the FPD6 and FPMI3 interactions in Ref. [1]. In addition, it has now also been shown that good agreement with experiment is also obtained for other important observables, namely spectroscopic factors for single-nucleon transfer, electric quadrupole and magnetic dipole transition strengths, and Gamow–Teller strengths.

For spectroscopic factors the FPD6 interaction leads to improved general agreement with experiment compared to previous calculations. Good agreement is also obtained for the Gamow–Teller beta-decay matrix elements using a quenching factor of 0.629 for the $B(\mathrm{GT})$ values. We have calculated several GT distributions in the lower fp shell which, in view of the sparseness of measured distributions, can serve as a guide for further experiments.

The results obtained with the FPD6 interaction are generally very similar to those obtained with the model-independent FPMI3 interaction, but are somewhat better as regards particular details, such as for magnetic dipole transitions, and for masses 48 and 49 in general. The results of Ref. [1], together with the present results, constitute a validation of the reliability of both our model-dependent (FPD6) and model-independent (FPMI3) interactions, with FPD6 being the preferred interaction on the whole.

Work has also been carried out to investigate the applicability of the semi-empirical MSOBEP and the linear combination method in a truncated model space consisting of configurations of the form $0f_{7/2}^{n}(1p_{3/2}0f_{5/2}1p_{1/2})^{m}+0f_{7/2}^{n-1}(1p_{3/2}0f_{5/2}1p_{1/2})^{m+1}$, leading to much lower basis dimensions, which allows one to include some 500 levels and nuclei up to $A = 66$ in the fits. The results will be reported elsewhere [32].

References

[1] W.A. Richter, M.G. van der Merwe, R.E. Julies and B.A. Brown, Nucl. Phys. A 523 (1991) 325.
[2] B.A. Brown, W.A. Richter, R.E. Julies and B.H. Wildenthal, Ann. Phys. 182 (1988) 191.
[3] A. Etchegoyen, W.D.M. Rae, N.S. Godwin, W.A. Richter, C.H. Zimmerman, B.A. Brown, W.E. Ormand and J.S. Winfield, MSU–NSCL report 524 (1985).
[4] P.M. Endt, At. Data Nucl. Data Tables 19 (1977) 23.
[5] P.J. Brussaard and P.W.M. Glaudemans, Shell model applications in nuclear spectroscopy (North-Holland, Amsterdam, 1977).
[6] T.W. Burrows, Nucl. Data Sheets 40 (1983) 149.
[7] T.W. Burrows, Nucl. Data Sheets 48 (1986) 1.
[8] T.W. Burrows, Nucl. Data Sheets 48 (1986) 569.
[9] J.B. McGrory, B.H. Wildenthal and E.C. Halbert, Phys. Rev. C 2 (1970) 186.
[10] T.H. Olsen and E. Osnes, Phys. Norv. 8 (1975) 85.
[11] B.J. Cole, S. African J. Phys. 4 (1981) 5.
[12] B.J. Cole, J. Phys. G 7 (1981) 173.
[13] T.T.S. Kuo and G.E. Brown, Nucl. Phys. A 114 (1968) 241.
[14] T.T.S. Kuo and E. Osnes, Nucl. Phys. A 205 (1973) 1.
[15] J.B. McGrory, Phys. Rev. C 8 (1973) 693.
[16] P.M. Endt and C. van der Leun, Nucl. Phys. A 310 (1978) 1.
[17] S. Saini and M.R. Gunye, Phys. Rev. C 18 (1978) 2749.
[18] B.J. Cole, J. Phys. G 11 (1985) 961.

[19] Y.K. Gambhir, S. Hag and J.K. Suri, Phys. Rev. C 25 (1982) 630.
[20] P.M. Endt, At. Data Nucl. Data Tables 55 (1993) 171.
[21] P.M. Endt, At. Data Nucl. Data Tables 23 (1979) 3.
[22] B.J. Cole, J. Phys. G 11 (1985) 953.
[23] T.W. Burrows, Nucl. Data Sheets 45 (1986) 557.
[24] L. Zamick and G. Ripka, Nucl. Phys. A 116 (1968) 234.
[25] H. Miyatake, K. Ogawa, T. Shinozuka and M. Fujioka, Nucl. Phys. A 470 (1987) 328.
[26] B.H. Wildenthal, M.S. Curtin and B.A. Brown, Phys. Rev. C 28 (1983) 1343.
[27] D.H. Wilkinson and B.E.F. Macefield, Nucl. Phys. A 232 (1974) 58.
[28] P.M. Endt, Nucl Phys. A 521 (1990) 1.
[29] B.H. Wildenthal, Prog. Part. Phys. 11 (1984) 5.
[30] J. Honkanen, V. Koponen, H. Hyvönen, P. Taskinen, J. Äystö and K. Ogawa, Nucl. Phys. A 471 (1987) 489.
[31] W.A. Richter, M.G. van der Merwe, R.E. Julies, B.A. Brown, Shell model and nuclear structure, ed. A. Covello (World Scientific, Singapore, 1989) p. 149.
[32] M.G. van der Merwe, W.A. Richter and B.A. Brown, unpublished.